Journal of Chemical Health Risks

www.jchr.org

JCHR (2024) 14(5), 1641-1652 | ISSN:2251-6727

Response Surface and Artificial Neural Network Approach for Optimization and Kinetic Study of Acid Blue 113 (AB 113) Degradation Using Fe-N-Tio$_2$ Under Visible Light

Dhegam Srujana[1]*, Chintha Sailu[2], Thati Jyothi[3] and Pengonda Hari Babu[4]

[1,2,3,4] *Dept. of Chemical Engineering, University College of Technology, Osmania University, 500007, Telangana, India*

Corresponding Author: Dhegam Srujana,

(Received: 11 June 2024 Revised: 16 July 2024 Accepted: 10 August 2024)

KEYWORDS

Photocatalyst, Response surface Methodology, Artificial Neural Network, degradation and kinetic model

ABSTRACT:

Introduction: Industrialization, modernisation globalisation leading to pollution of water bodies. The major sources of contamination are textile industries. The removal of colour matters and treating coloured waste water with prominent technologies Advanced Oxidation Process with utilisation of renewable energy like solar energy is more viable and efficient than other conventional technologies like, filtration, coagulation and membrane separation etc.

Objectives: Removal and kinetic study of textile dye with utilization of solar spectra for degradation of Acid Blue 113(AB 113) using Fe-N-TiO_2.

Methods: The investigation of synthesized photocatalyst Fe-N-TiO_2 by various characterization techniques like, XRD, SEM, FTIR, UV-DRS and XPS. Photocatalytic batch experiments with design of experiment on three process variables (concentration, pH and reaction time) were modelled by RSM-CCD and experimental variables optimized. were conducted. The system response determined using MINITAB (statistical software) and MATLAB. Kinetics of the system determined using Langmuier-Hinshel wood model.

Results: The co-doping mechanism lead to reduce the band gap to 2.6ev and the optimum conditions for AB113 are concentration (19mg/l), pH (5) and reaction time (180min) with degradation is 91.1% predicted through analysis of variance (ANOVA). Outcomes RSM-CCD of The predicted models with observed response significance were compared in terms of coefficient of determination, R^2= 0.9662 for RSM model and R^2 = 0.9516 for ANN model for AB113.and the op The kinetics of degradation of AB 113 followed first-order rate constants (k) by Langmuir–Hinshelwood (L–H) kinetic model at different pH levels are as follows: 1.049 min^{-1} at pH 5, 0.752 min^{-1} at pH 7, and 0.45 min^{-1} at pH 9.

Conclusions: The outcomes obtained in this study are commercially valuable for textile waste water treatment in real time firms. Using solar light for degradation of harmful textile dyes is viable sustaining environment and real time data can be achieved by utilizing statistical techniques like, RSM-CCD-ANN.

1. Introduction

At present times, contamination of water resources is one of the global concerns [1] by run-off coloured wastewater from distinguished industries like, paper, pulp, cosmetics, textiles, food and printing etc. This results a toxic ecosystem by severely affecting the plant, aquatic and human personal by causing nausea, irritation, cancer and sometimes leads to death [2]. To maintain the sustainable and clean water bodies, it is essential to eliminate the colored matters (dyes) through

Journal of Chemical Health Risks

www.jchr.org

JCHR (2024) 14(5), 1641-1652 | ISSN:2251-6727

the appropriate technologies by degradation of wastewater discharged from textile industries remarkably at large which are the dominant contributors among the industries [3]. Advanced Oxidation Process (AOP) is the one of the expedient technology for the removal of dye molecules by converting them into CO_2, salts and water which stands on the production of hydroxyl radicals (OH.) [4][[5]. Among the various combinations of AOPs, AOP with heterogeneous photocatalysis is the most prominent combination [6] to remove the coloured dyes from textile wastewaters. In general, semiconductors like TiO_2 materials are globally preferable photocatalysts for production of hydroxyl radicals by photo-catalyzed reactions due to their abundance and virtue of properties like thermal stability, electronic configuration, non-toxic, chemical resistant and band gap (3.2eV) [7]. However, TiO_2 is incapable of absorbing visible light spectrum from the solar light due to its wide optical band gap. To overcome this short coming, it's essential to alter the electronic structure of TiO_2 by employing doping method [8]. Many researchers suggested with the better results by employing co-doping approach to dial down the band gap to utilize the solar light rather the single doping mechanism [9]. Amidst of combinations of dopants, a metal (Fe) with non-metal(N) co-doping would be the better approaching mechanism for reduction of band gap TiO_2 where, Fe isomorphically replaces Ti4+ ions with Fe^{+3} in TiO_2 and Nitrogen(N) p-states mixes with Oxygen(O) 2p states which results narrowing in the band gap[10].

2. Objectives

This study concentrated on the removal of azo dye Acid Blue 113 shown in Fig.1 by using Fe-N-TiO_2 catalyst under solar radiation to obtain the optimized values of various factors like type of dye concentration, pH and reaction time by using most prominent Response Surface Methodology (RSM) and Artificial Neural Network (ANN) [11]. RSM is an empirical statistical modelling approach to build the design of experiments (DOE) involving with numerous factors and an Artificial Neural Networks(ANN) is the one of the branch of machine learning algorithm which emulate the human neuron[12][13]. This work employed the Central Composite Design (CCD) based RSM and ANN prediction models to evaluate the process with 3 factors on 2 levels (2^3).

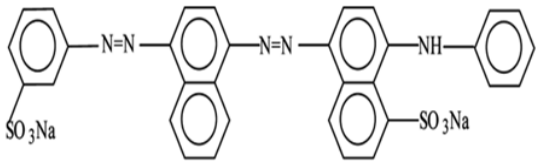

Fig.1. Acid Blue 113, λmax=566nm

3. Materials & Methods

Reagents and Chemicals

Titanium tetra (IV) Isopropoxide (TTIP) procured from Sigma-Aldrich, Iron (III) Nitrate nano hydrate Fe(NO3)3.9H2O, Urea (NH_2CONH_2) purchased from Isochem and Glacial Acetic Acid, hydrochloric acid(HCl), NaOH, Absolute Ethanol (99.9% pure), Double distilled water (DDW) of analytical grade were directly utilized and Acid Blue 113 ($C_{32}H_{21}N_5Na_2O_6S_2$, M.W. = 681.65 $gmol^{-1}$) used for degradation studies.

Synthesis of Photocatalyst

An alkoxide precursor Titanium tetra isopropoxide (TTIP) and absolute ethanol were mixed in 1:3 volume ratios under constant mixing for 60 min. To this solution, an aqueous ammonia solution of 0.32 M with 3wt% of Iron (III) Nitrate nano hydrate and 1ml of glacial acetic acid were added drop wise under vigorous mixing for 60 min. The obtained precipitate aged for 12 hrs and dried for 2hrs at 120°C. The resultant sample was subjected to calcination at 400°C with a rate 4°C/min for 1hr.

Catalyst Characterization

The crystalline structure of synthesized catalyst were studied using X-ray diffraction (XRD) technique on Rigaku X-Ray Diffractometer by using Ni-filtered Cu Kα radiation (λ = 1.5406 A°) in the range of 2θ= 10°-80° with 0.02°/2θ step size with 40 kV and 30 mA of operating conditions of accelerating voltage and current respectively. To evaluate the morphology Scanning electron microscopy (SEM) (JSM-7800F), to diagnose functional groups FTIR-8400S, SHIMADZU were used. And to determine the optical band gap UV-Vis Diffuse Reluctance (UV-Vis DRS) Spectra (Hitachi U-3900 spectrometer) used based on the reference (BaSO4 standard) in the range of 200-1000nm. X-ray photoelectron spectroscopy (XPS) was carried out for

Journal of Chemical Health Risks
www.jchr.org
JCHR (2024) 14(5), 1641-1652 | ISSN:2251-6727

elemental analysis using monochromatic Al-K radiation at chamber pressure of 10-8 mbar and ambient temperature on a K-alpha Thermo Fisher Scientific Spectrometer.

Photocatlytic Experiments

Synthetic wastewater & Photocatalytic experiments

The Photocatalytic Experiments were carried on batch process with 250ml of dye solution with concentrations based on design of experiments with constant catalyst (Fe-N-TiO_2) loading of 1mg/250ml of dye solution. Experiments were performed in solar light under a continuous vigorous stirring of 350rpm. Prior to photocatalytic experiments, the sample solutions were placed in dark to establish equilibrium between dye solution and catalyst. 10ml of samples were collected at 30, 105 and 180 min of reaction time and were analysed through UV-Visible Spectrophotometry. The colour removal of dye solution was determined as follows:

$$\%Degradation = \frac{C_0 - C}{C_0} \times 100$$

Where, C_0 and C are the initial and final concentration values of samples at any time respectively.

3.5 Statistical approach for Optimization

3.5.1 Design of Experiments (DOE)

The Response surface Methodology (RSM) approach is employed to draw the influence of various independent parameters on system response. RSM is familiar statistical method to depict the number of experiments and to analyse the validation of the model by correlating the experimental design results with the predicted results. Dye concentration (AB113), pH and time of reaction with catalyst dosage of 1g/250ml on colour removal efficiency were investigated. Central Composite Design (CCD) at two levels involving three parameters as shown in Table 1.

Table 1: Executing levels of independent parameters with RSM- CCD-DOE approach.

S. No.	Independent factor	Low level (-1)	High level (+1)
1.	Dye Concentration(mg/l)	10	50
2.	pH	5	9
3.	Time of reaction(min)	30	180

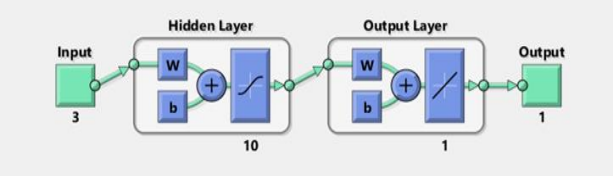

Fig.2.ANN input –hidden-output network architecture for AB113

By using RSM-CCD-DOE, a number of 20 factorial designated experiments were generated by conducting the process at 2 levels with 3 factors and were displayed in Table 2. The dye solution was prepared with AB113 and the reaction time was varied between 30-180 min to evaluate the process performance. The independent factors were labelled as X_1, X_2, and X_3 respectively. The %degradation response was assessed by investigating the influence of process variables. During the design of experiments five replications were considered to obtain a better estimate of experimental errors [14]. To uphold the validation of experiments, a quadratic model was established which is given by

$$Y=B_0+B_1X_1+B_2X_2+B_3X_3+B_{11}X_{12}+B_{22}X_{22}+B_{33}X_{32}+ B_{12}X_1X_2 + B_{13}X_1X_3 + B_{23}X_2X_3$$

Where, Y: Predicted response % degradation, B0: Constant coefficient, B_{11}, B_{22} and B_{33}: quadratic coefficients, B_{12}, B_{13} and B_{23}: Interaction coefficients respectively. X_1, X_2, and X_3 are coded notations of independent factors [15].

3.6 Artificial Neural Network (ANN)

The artificial neural network (ANN) tailored from MATLAB version 2019b used a computational technique to substantiate the correlation among the input and output variables and to develop a predictability regression of handling data [16]. ANN responses rely on empirical facts like the behaviour of human neuron nerve network. In this paper, to quantify the non-linear relation between input and output obtained from statistical response surface methodology (RSM) were trained by ANN algorithm. By utilizing the nftool, data trained and compared the response from

Journal of Chemical Health Risks
www.jchr.org
JCHR (2024) 14(5), 1641-1652 | ISSN:2251-6727

ANN with that of RSM. An architecture of artificial neural network (ANN) with input layer of 3 nodes (Concentration, pH and reaction time) with output layer of 1 node (%degradation) with 10 neurons are in hidden layer for each dye. The Fig.2 represents the ANN input-hidden-output network architecture for AB 113.

3.7 Reaction Kinetics

The degradation rate relies on the mass transfer of adsorbed molecules and the rate of reaction on the catalyst surface. Henceforth the catalyst surface maintained with adequate mixing of dye solution slurry during batch process. The kinetics was determined by fitting a Langmuir–Hinshelwood (L–H) kinetics model.

$$-r_{dye} = \frac{kKC}{1+KC}$$

Where: $-r_d$ rate of disappearance of dye molecule

C is concentration of dye solution, k is the kinetic degradation rate constant and K represents the equivalent adsorption coefficient.

4. Results & Discussion

XRD study

Calcined catalyst samples were subjected to X-Ray Diffraction technique. The XRD pattern of Fe-N-TiO_2 shown in Fig.3 reveals the dopants elements (N, Fe) into the TiO_2 crystal. The resultant peaks at 2θ= 25.37 (101), 37.98 (004), 48.1(200), 54.06(105), 55.1(221), 62.7(204), 68.9(116), 70.3(220) and 75.27(215) were concurred with the standard values of JCPDS NO. 00-21-1272. The broadness and shortness of peaks at higher angles due the inclusion of dopants. The successive peaks obtained at 54.06 and 55.1 are might be a narrow change in the structural lattice due to replace of O with N and Ti with Fe [17].The average crystallite size (D) can be obtained from Debye-Scherrer Equation as shown in below:

$$Crystallite\ Size(D) = \frac{k\lambda}{\beta cos\theta}$$

Where, k is lattice constant =0.9, λ =0.15406nm which is the corresponding wavelength of line Cu-Kα, β is the full width at half maximum (FWHM) at various diffraction angles (2θ). By using the Debye-Scherrer equation, the crystallite size (D) = 8.9nm and lattice parameters a=4.073A^o and c=9.17A^o with cell volume of 152.18nm3are determined. The obtained a and c are very close to the lattice parameters of bulk tetragonal anatase phase of JCPDS No.21-1272, a=3.87852A^o and c=9.51139A^o [18]. The slight deviations in increase of a and decrease in c are due to reduction in Ti-O-Ti bond length henceforth contraction of lattice resulted due to formation of oxygen vacancies by introducing the dopants[19].

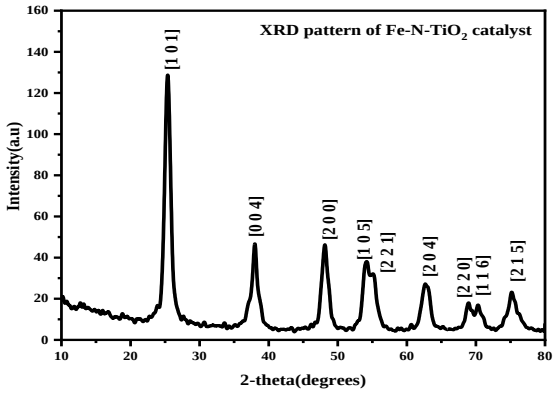

Fig.3 XRD pattern of Fe-N-TiO_2

SEM study

The surface morphology of prepared Fe-N-TiO_2 catalyst by sol-gel method has been investigated using Scanning Electron Microscopy(SEM) and is shown in Fig.4(a) & Fig.4(b) which explores the spherical structure and agglomeration which may be attained by the Co-doping of Fe content to N-TiO_2. The particles distribution in the sample fitted by the Normal distribution and the average size and average area of particle were 756nm and 220nm^2.

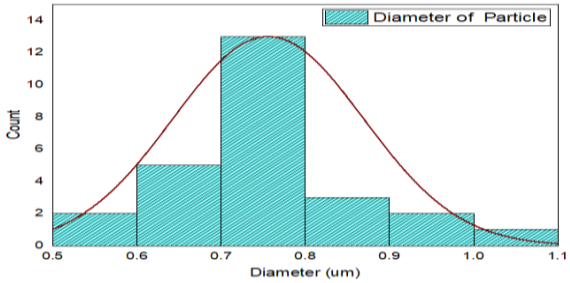

Fig.4(a). Normal distribution of diameter of Fe-N-TiO_2 catalyst particles

Journal of Chemical Health Risks
www.jchr.org
JCHR (2024) 14(5), 1641-1652 | ISSN:2251-6727

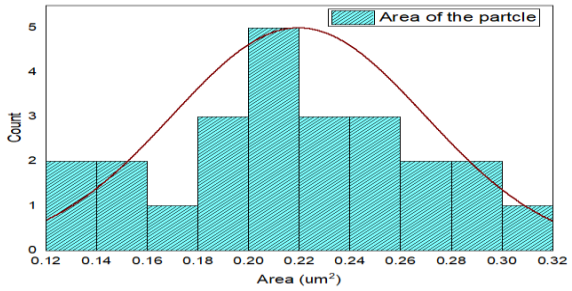

Fig.4(b).Normal distribution of area of Fe-N-TiO_2 catalyst particles

FTIR study

The results obtained from the Fourier Transform of Co-doped Fe-N-TiO_2 shown in Fig.5 which shown a characteristic wide region 500-930cm^{-1} referred to vibrations between Ti-O stretching and O-Ti-O or Ti-O-Ti framework bonds. The O-H bending and vibrations observed in the regions of 1628-1710cm^{-1} and 3000-3400cm^{-1} where O-H vibrations are responsible for the absorption water molecules on to TiO_2 surface during sol-gel synthesis of catalyst[8]. The doped element Fe evident the Fe-O bond vibration observed in between 520-640cm^{-1} and Ti-N vibrations in the TiO_2 lattice appeared the peak in between 1000-1136cm^{-1} [20].

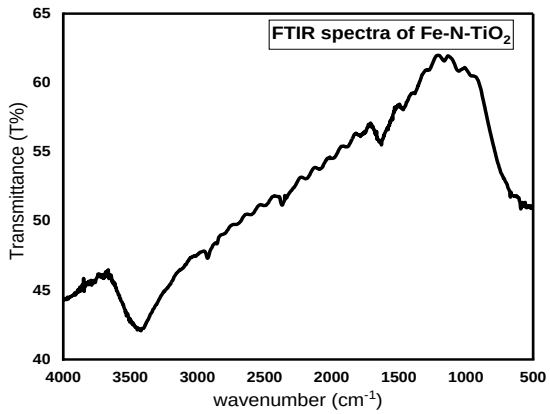

Fig. 5 FTIR spectra of Fe-N-TiO_2

UV-DRS

The UV-DRS spectra of Fe-N-TiO_2 was shown Fig.6(a).the figure indicates the absorption edge came into view of longer wavelength which is at 550 nm. The shift of absorption spectra towards visible region is due by incorporation of cation (Fe^{+3}) and Anion (N^{-3}) and also due to the exchange of d-orbital electrons between Fe and Ti. The band gap of synthesized Fe-N-TiO_2 can be determined by using Tauc plot which is a graphical method to plot the graph between αhν and $A(h\nu-E_g)^{n/2}$ where, α is the absorption coefficient, hν is the photon energy, n~1 for direct transition between bands and Eg is the band gap energy. From the Fig.6 (b) it's been found that the band gap of co-doped Fe-N-TiO_2 is 2.6eV. The dial down of energy band gap from 3.2eV (TiO_2) to 2.6eV (Fe-N-TiO_2) might be caused by overlapping of d-orbitals of Ti^{+4} and Fe^{+3}. On the flip side, doping with Nitrogen leads to formation of intermediate energy levels by mixing the N-2p orbitals with O-2p Orbitals [21].

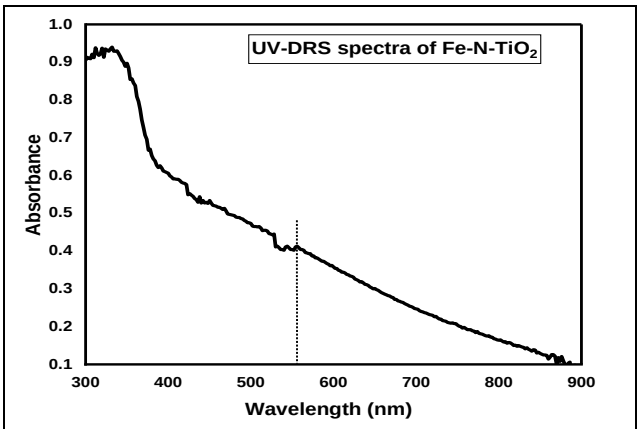

Fig.6 (a) UV-DRS spectra of Fe-N-TiO_2

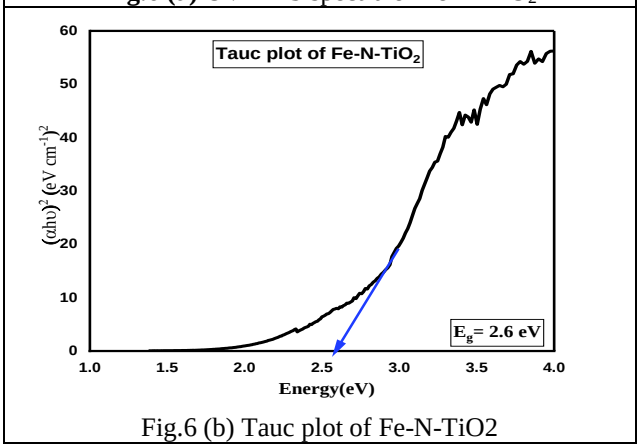

Fig.6 (b) Tauc plot of Fe-N-TiO2

XPS

The figure explored the xps survey of components presented in the synthesized Fe-N-TiO_2. The peaks at 458eV, 462eV are the binding energies of Ti 2p1/2, Ti 2p3/2 and peak at 530eV is the binding energy of O1s. The peaks at 404eV is the binding energy of the N1s which attributes the N-Ti-O linkages and at 709eV [10] describes the Fe2p which indicates the incorporation of

Journal of Chemical Health Risks

www.jchr.org

JCHR (2024) 14(5), 1641-1652 | ISSN:2251-6727

Fe into the TiO_2 lattice by substitution of Ti^{+4} by Fe^{+3} ion as the ionic radius of Fe^{+3} (0.64A°) is less than that of Ti^{+4}(0.68A°) [22].

Response Surface Analysis

Numerical Optimization was performed Minitab 19 software's CCD was adopted to analyze RSM model with the concept of ANOVA (Analysis of Variance) by examining the linear, quadratic and two-factor interactions to describe the correlation between output and input variables as response % degradation of YAB113 for AB 113.Table.2 explore the three-factor CCD quadratic statistical model in coded factors.

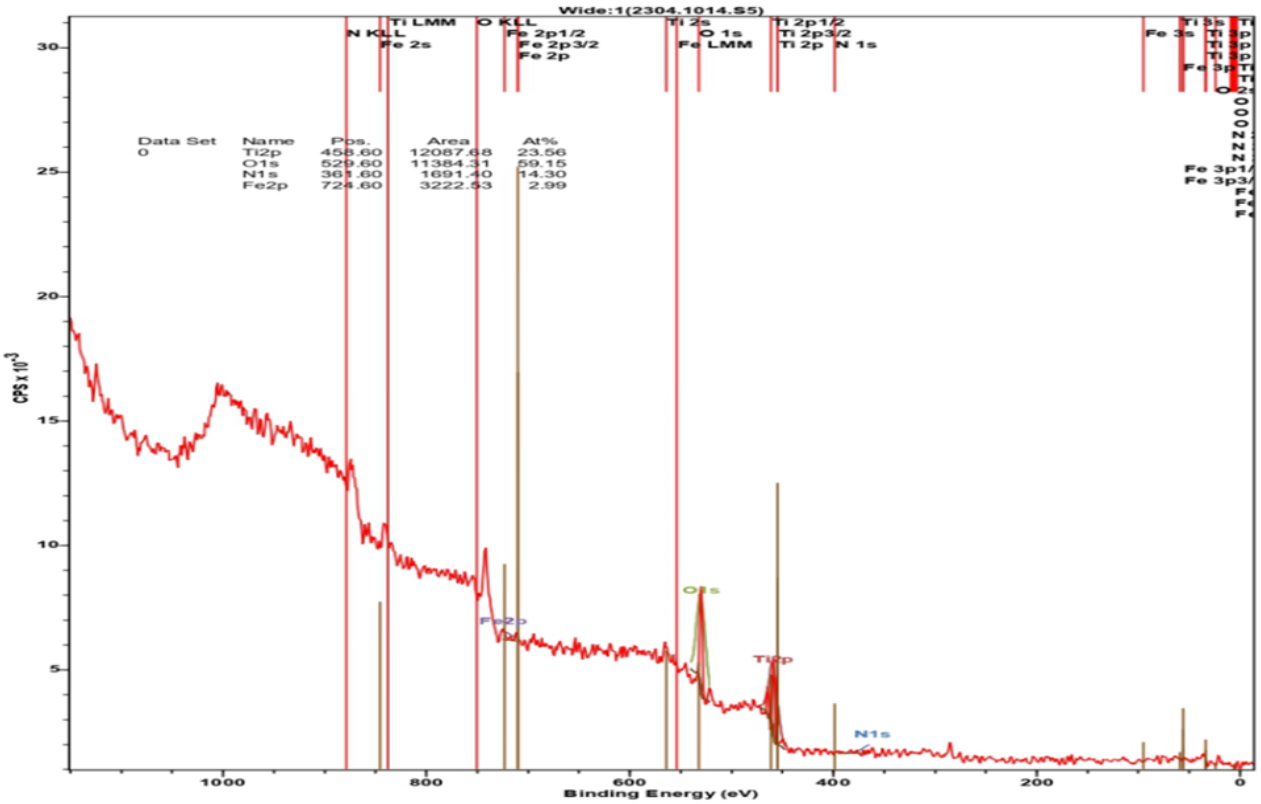

Fig.7.XPS spectra of Fe-N-TiO_2

Table. 2 Three-factor RSM-CCD design

Run No.	X_1	X_2	X_3	$Y_{AB\ 113}$ (% Degradation of AB113)		
	Concentration	pH	Reaction time	Obs.	Pred.(RSM)	Pred.(ANN)
1	10	5	30	20.2	24.06	20.7
2	50	5	er30	16.5	19.57	16.82
3	10	9	30	15.0	17.27	15.03
4	50	9	30	10.0	10.88	9.74
5	10	5	180	89.0	89.16	89.15
6	50	5	180	70.5	69.27	70.72
7	10	9	180	66.0	63.97	66.48

Journal of Chemical Health Risks

www.jchr.org

JCHR (2024) 14(5), 1641-1652 | ISSN:2251-6727

8	50	9	180	45.0	42.18	44.72
9	10	7	105	65.0	60.73	64.93
10	50	7	105	47.5	47.59	48.42
11	30	5	105	75.0	69.14	73.67
12	30	9	105	50.5	52.2	50.46
13	30	7	30	40.0	29.92	19.08
14	30	7	180	72.2	78.12	72.84
15	30	7	105	65.0	63.4	62.72
16	30	7	105	58.1	63.4	62.72
17	30	7	105	65.0	63.4	62.72
18	30	7	105	60.0	63.4	62.72
19	30	7	105	59.0	63.4	62.72
20	30	7	105	65.0	63.4	62.72

Statistical analysis of response model

The modelled response in terms of equation defined by YAB113 (%degradation of AB113). The factor coefficient reveals the synergic effects on the response of the system. Where, positive coefficients are responsible to conducive response and negative coefficients are detrimental towards response of the system (%degradation).The developed model equations in terms of coded factors are expressed as,

Y=63.406.57 concentration-8.47 pH
+ 24.10 reaction time-9.24 concentration*concentration
– 2.74 pH*pH- 9.39 reaction time*reaction time–
0.47 concentration*pH-
3.85 concentration*reaction time–
4.60 pH*reaction time

Analysis of Variance (ANOVA)

The validation of the model can be predicted by using of Analysis of Variance (ANOVA) with the P-values <0.05 from F-test while the confidence level of 95% employed during probability analysis of significance of the regression model. The ANOVA results of dye solution (AB113) were reported in the Table.3. From the obtained results of ANOVA of dye all the main interactions are significant and most of the one-way and two-way interactions are insignificant and analysis of R2 (coefficient of determination) also reported as R2AB113 =0.9674 respectively. High value in R2 prevails good fitness of proposed models with experiment results [23]. The Fig. 8 shows a great correlation between the observed (experimental) response and predicted response by RSM for the degradation of the dye as the data sets are lined up near to the diagonal line.

Response 3D and 2D contour plots

The interaction effects of individual and combining the input variables (Concentration, pH and reaction time) on the output response (AB113) are examined through 3-D response plots. The %degradation of dye plotted against two variables while keeping the other variables to be constant shown from Fig 9(a) to Fig. 9(c).

The contour plots shown in Fig. 10 for the dye AB113 explains the main effects of the input variables of the output response (%degradation). From Fig.10 the AB113 degradation achieved maximum with low pH (<6.5) at low concentration range (<25mg/l) and high reaction time (>150 min). Consequently minimum degradation achieved at high pH (>8) at high concentration range (>45mg/l) and reaction time (<50min). It might be due to the dyes are anionic and in acidic environment leads to more adsorptions of dye molecule on to positively charged catalyst surface. The vice versa observed at higher pH range(basic) medium with positively charged catalyst surface due to minimal adsorption onto catalyst surface. Higher the reaction time provides sufficient time of contact for oxidation and reduction reactions of dye molecules with generated hydroxyl radicals. Eventually, higher the concentration of dye solution leads to lower the degradation due to

Journal of Chemical Health Risks

www.jchr.org

JCHR (2024) 14(5), 1641-1652 | ISSN:2251-6727

insufficient catalyst particle surface and penetration of light through the thick environment of dye solution.

The pareto chart of dye shown in Fig. 11 indicates the synergic effect of input variable on output response. The dyes degrade by major contribution of reaction time and pH of the solution.

Numerical response optimization and validation of model& Kinetic Study

To maximize the degradation of dyes, input variables (concentration, pH and reaction time) were held in the optimum range of the design space by using the numerical optimization technique with desirability of 1. The Fig. 12 Shows the plot of best optimum

Table.3 Analysis of Variance (ANOVA) of AB113

Source	DF	Adj SS	Adj	F	P	Remarks
Model	9	8977.26	997.47	32.95	0.000	Significant
Linear	3	6957.16	2319.05	76.61	0.000	Significant
Concentration	1	431.65	431.65	14.26	0.004	Significant
pH	1	717.41	717.41	23.70	0.001	Significant
reaction time	1	5808.10	5808.10	191.86	0.000	Significant
Square	3	1730.44	576.81	19.05	0.000	Significant
Concentration*concentration	1	234.60	234.60	7.75	0.019	Significant
pH*pH	1	20.59	20.59	0.68	0.429	In Significant
reaction time*reaction time	1	242.29	242.29	8.00	0.018	Significant
2-Way Interaction	3	289.66	96.55	3.19	0.071	In Significant
concentration*pH	1	1.80	1.80	0.06	0.812	In Significant
Concentration*reaction time	1	118.58	118.58	3.92	0.076	In Significant
pH*reaction time	1	169.28	169.28	5.59	0.040	Significant
Error	10	302.72	30.27			
Lack-of-Fit	5	247.51	49.50	4.48	0.063	Significant
Pure Error	5	55.21	11.04			
Total	19	9279.98				

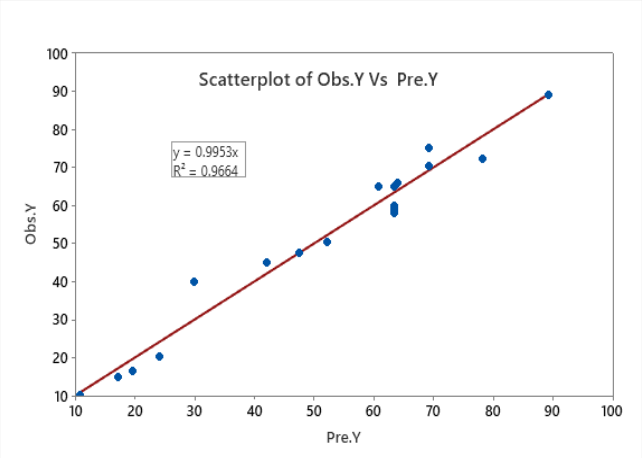

Fig.8. Regression plot of Obs.Y vs Pre.Y for AB113

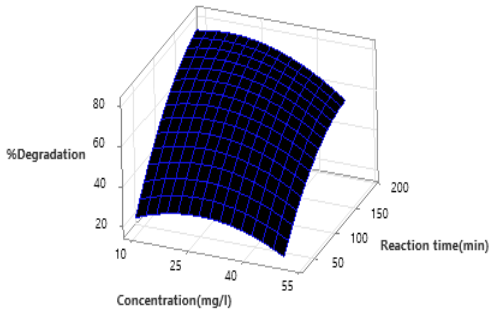

Fig. 9(a) surface plot of %degradation (AB113) Vs Concentration (mg/l), reaction time(min)

Journal of Chemical Health Risks
www.jchr.org
JCHR (2024) 14(5), 1641-1652 | ISSN:2251-6727

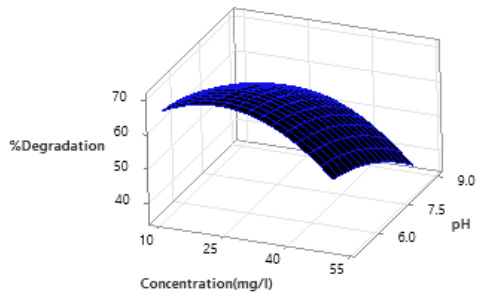

Fig. 9(b) surface plot of %degradation (AB113) Vs Concentration (mg/l), pH

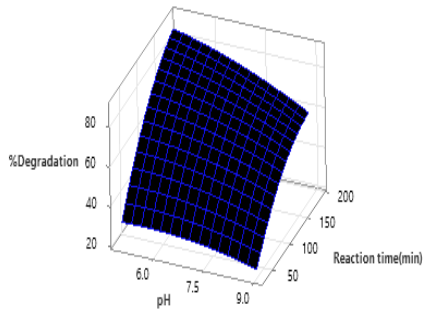

Fig. 9(c) surface plot of %degradation (AB113) Vs pH, reaction time (min)

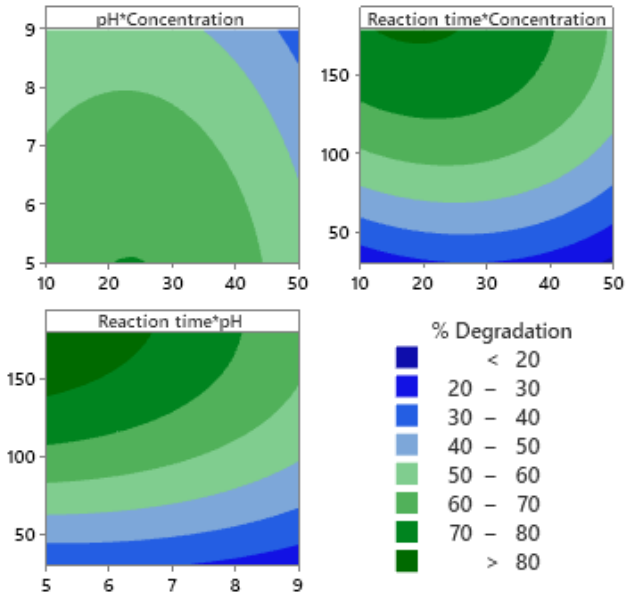

Fig.10. Contour plots of %Degradation of AB113

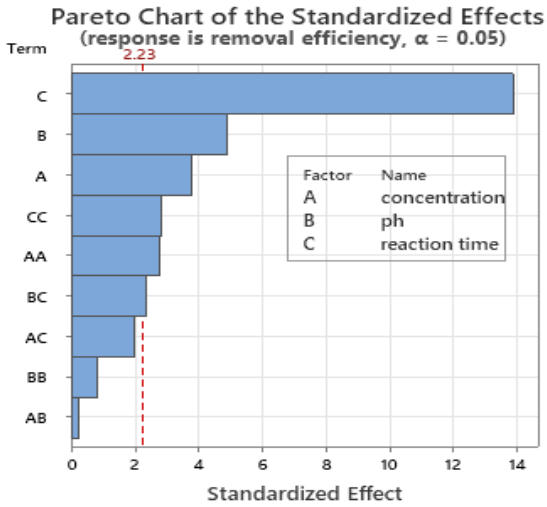

Fig. 11. Pareto chart of AB113

Conditions for AB113 are concentration (19mg/l), pH (5) and reaction time (180min) with output response is 91.1%. With optimum conditions, it is required to conduct an extra set of experiment to ascertain the validation and accuracy of the predicted model [24]. Table.4 reveals that, the experimental results from extra set at optimum conditions are lined with good agreement with the predicted values by RSM model.

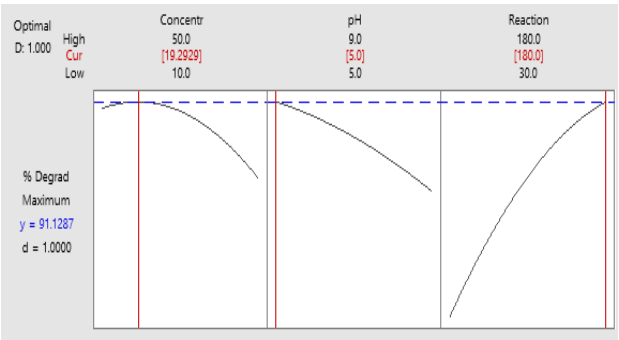

Fig.12.Response optimizer plots for AB113 by numerical optimization technique.

Journal of Chemical Health Risks

www.jchr.org

JCHR (2024) 14(5), 1641-1652 | ISSN:2251-6727

Study of modelling by Artificial Neural Network (ANN)

The ANN architecture (3:10:1) with Bayesian regularization named MATLAB function (trainbr) at the hidden layer was used to model the % degradation of dye as a response. The nftool used to train and test the data to identify the correlation between the input and output parameters and the output response data by ANN are included in Table.2. The trained regression shown in Fig. 13 explored the best coefficient determination R^2=0.9701 for AB113.

Table.4. Confirmation of validation of model by RSM-CCD with experimental results

Dye	RSM Predicted values (%)	Experimental values (%)
AB113	91.12	90.02

Comparing the RSM and ANN results

The accuracy of results obtained by RSM and ANN were explained by the fitting of best correlation coefficient for non-linear expressions of response. The Fig.14 shown the plot of comparing the results obtained from experimental, predicted RSM and ANN output. Both RSM and ANN were coincided with experimental (observed)values. However the scope and accuracy of ANN would be greater than RSM when the predicted model involved with more non-linearity with higher order of polynomial expressions [24].

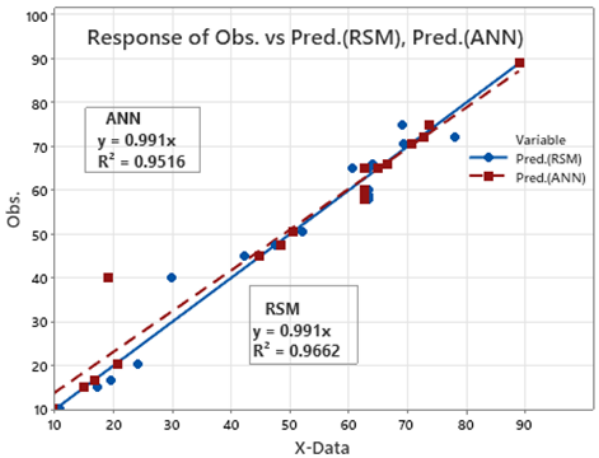

Fig.14. Regression plot of Observed response vs Predicted (RSM & ANN) for AB113

Kinetic Study

The plot of the reciprocal of the degradation rate (-1/rd) with the reciprocal of the concentration (1/C) at various levels of pH=5,7and 9 drawn using Langmuir–Hinshelwood (L–H) kinetics model with first order reaction rate as shown in the Fig.15 yield the parameters K and k for the photocatalytic degradation of the dye solution obtained from the slope and the intercept and the values of K and k [25] are shown in Table.5. The values are clearly indicating that the reaction rate constants at all operated pH levels are much greater than adsorption constant. And among the rate of reactions, the rate at lower pH (5) is more than greater values of pH where the surface conditions are facilitated to adsorb the negative dye molecules towards the positive catalyst surface.

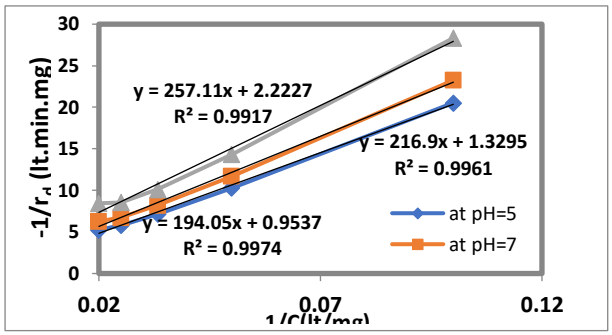

Fig. 15. Plot of 1/C Vs -1/r_d

Table.5. values of adsorption and rate constant of degradation of dye at various pH levels

	At pH=5		At pH=7		At pH=9	
	K (lt/mg)	k (min^{-1})	K (lt/mg)	k (min^{-1})	K (lt/mg)	k (min^{-1})
AB 113	0.0051	1.049	0.0046	0.752	0.0039	0.45

Conclusion

In this study the synthesis of Fe-N-TiO_2 as co-doped catalyst for the treatment of textile binary dye solution was found successful by examining the catalyst with various characterization techniques like, XRD, SEM, FTIR, UV-DRS and XPS. The broadness of the peaks at

Journal of Chemical Health Risks

www.jchr.org

JCHR (2024) 14(5), 1641-1652 | ISSN:2251-6727

higher angles in XRD pattern, shifting the absorption spectra towards visible region in UV-DRS spectra and atomic percentage of Ti, O, Fe and N using XPS spectra confirmed the successful co-dopants into parental TiO_2 lattice. The use of Fe-N-TiO_2 in AB113 dye solution achieved good percentage degradation under solar light. By using design of the experiment, RSM and predicted model response for the dye validated by evaluating system response at optimum conditions (concentration (19mg/l), pH (5) and reaction time (180min) with output response is 91.1% for AB113) which are determined using numerical optimization technique. The set of design of experiments evaluated by using artificial neural network (ANN) using MATLAB trainbr as function. The predicted model by RSM and ANN were significant with observed response with $R^2 > 0.95$. The rate of degradation of AB113 followed first order reaction kinetics and lower pH is favorable for higher the degradation (at pH=5, k=1.049). The results obtained in this study are commercially valuable for textile waste water treatment in real time firms. Using solar light for degradation of harmful textile dyes is viable sustaining environment and real time data can be achieved by utilizing statistical techniques like, RSM for quadratic expressions. For the higher order degree of polynomial ANN will provide the best correlation among the input and output variables. The adoption of computation techniques into experimentation will enhances real time performance and reduces the cost of the process.

Acknowledgement

This work is done by the support of Department of Chemical Engineering, University of College of Technology (OUCT), Osmania University, Hyderabad. And Department of Chemical Engineering and Chemistry, RGUKT-Basar.

References

[1] T. Hey, N. Bajraktari, J. Vogel, C. Hélix Nielsen, J. la Cour Jansen, and K. Jönsson, "The effects of physicochemical wastewater treatment operations on forward osmosis," *Environ. Technol. (United Kingdom)*, vol. 38, no. 17, pp. 2130–2142, 2017, doi: 10.1080/09593330.2016.1246616.

[2] Y. Pan, J. Wang, C. Sun, X. Liu, and H. Zhang, "Fabrication of highly hydrophobic organic-inorganic hybrid magnetic polysulfone microcapsules: A lab-scale feasibility study for removal of oil and organic dyes from environmental aqueous samples," *J. Hazard. Mater.*, vol. 309, pp. 65–76, 2016, doi: 10.1016/j.jhazmat.2016.02.004.

[3] H. Gopalappa, K. Yogendra, K. M. Mahadevan, and N. Madhusudhana, "A comparative study on photocatalytic degradation of Violet GL2B azo dye using CaO and TiO2 nanoparticles," *Int. J. Sci. Res.*, vol. 1, no. 2, pp. 91–95, 2012, doi: 10.13140/RG.2.2.11328.17922.

[4] N. Noor Mohammadi, E. Pajootan, H. Bahrami, and M. Arami, *Magnetization of TiO2 nanofibrous spheres by one-step ultrasonic-assisted electrochemical technique*, vol. 265. Elsevier B.V, 2018. doi: 10.1016/j.molliq.2018.04.067.

[5] V. D. Gosavi and S. Sharma, "Journal of Environmental Science , Computer Science and Engineering & Technology A General Review on Various Treatment Methods for Textile Wastewater," *J. Environ. Sci. Comput. Sci. Eng. Technol.*, vol. 3, no. 1, pp. 29–39, 2014.

[6] E. K. Tetteh, S. Rathilal, D. Asante-Sackey, and M. N. Chollom, "Prospects of synthesized magnetic tio2-based membranes for wastewater treatment: A review," *Materials (Basel).*, vol. 14, no. 13, 2021, doi: 10.3390/ma14133524.

[7] A. Carabin, P. Drogui, and D. Robert, "Photo-degradation of carbamazepine using TiO2 suspended photocatalysts," *J. Taiwan Inst. Chem. Eng.*, vol. 54, pp. 109–117, 2015, doi: 10.1016/j.jtice.2015.03.006.

[8] L. Pirinejad, A. Maleki, B. Shahmoradi, H. Daraei, J.-K. Yang, and S.-M. Lee, "Synthesis and application of Fe-N-Cr-TiO2 nanocatalyst for photocatalytic degradation of Acid Black 1 under LED light irradiation," *J. Mol. Liq.*, vol. 279, pp. 232–240, 2019.

[9] X. Cao, C. Liu, Y. Hu, W. Yang, and J. Chen, "Synthesis of N/Fe comodified TiO2 loaded on bentonite for enhanced photocatalytic activity under UV-Vis light," *J. Nanomater.*, vol. 2016, p. 1, 2016.

[10] B. C. Hsu, S. S. Chen, C. Su, and Y. C. Li, "Preparation and characterization of nanocrystalline Fe/N co-doped titania," *Ferroelectrics*, vol. 381, no. 1 PART 2, pp. 51–58, 2009, doi: 10.1080/00150190902865069.

[11] M. Khayet, C. Cojocaru, and M. Essalhi, "Artificial neural network modeling and response surface methodology of desalination by reverse osmosis," *J. Memb. Sci.*, vol. 368, no. 1–2, pp. 202–214, 2011, doi: 10.1016/j.memsci.2010.11.030.

[12] M. Zulfiqar, M. F. R. Samsudin, and S. Sufian,

Journal of Chemical Health Risks

www.jchr.org

JCHR (2024) 14(5), 1641-1652 | ISSN:2251-6727

"Modelling and optimization of photocatalytic degradation of phenol via TiO2 nanoparticles: An insight into response surface methodology and artificial neural network," *J. Photochem. Photobiol. A Chem.*, vol. 384, p. 112039, 2019.

[13] S.-H. Han, K. W. Kim, S. Kim, and Y. C. Youn, "Artificial Neural Network: Understanding the Basic Concepts without Mathematics," *Dement. Neurocognitive Disord.*, vol. 17, no. 3, p. 83, 2018, doi: 10.12779/dnd.2018.17.3.83.

[14] J.-K. Park, G.-M. Lee, C.-Y. Lee, K.-B. Hur, and N.-H. Lee, "Analysis of Siloxane Adsorption Characteristics Using Response Surface Methodology," *Environ. Eng. Res.*, vol. 17, no. 2, pp. 117–122, 2012, doi: 10.4491/eer.2012.17.2.117.

[15] Y. P. Lin and M. Mehrvar, "Photocatalytic treatment of an actual confectionery wastewater using Ag/TiO2/Fe2O3: Optimization of photocatalytic reactions using surface response methodology," *Catalysts*, vol. 8, no. 10, pp. 1–17, 2018, doi: 10.3390/catal8100409.

[16] doi: 10. 1016/j. mex. 2019. 07. 016. y. A. Igwegbe, Chinen[1] C. A. Igwegbe et al., "Modeling of adsorption of Methylene Blue dye on Ho-CaWO4 nanoparticles using Response Surface Methodology (RSM) and Artificial Neural Network (ANN) techniques," MethodsX, vol. 6, pp. 1779–1797, 2019 *et al.*, "Modeling of adsorption of Methylene Blue dye on Ho-CaWO4 nanoparticles using Response Surface Methodology (RSM) and Artificial Neural Network (ANN) techniques," *MethodsX*, vol. 6, pp. 1779–1797, 2019, doi: 10.1016/j.mex.2019.07.016.

[17] H. Irie, Y. Watanabe, and K. Hashimoto, "Carbon-doped Anatase TiO2 Powders as a Visible-light Sensitive Photocatalyst," *Chem. Lett.*, vol. 32, no. 8, pp. 772–773, 2003, doi: 10.1246/cl.2003.772.

[18] I. Djerdj, A. M. Tonejc, and A. Tonejc, "Structural Refinement of Nanocrystalline TiO2 Samples," *Electron Crystallogr.*, no. Pw 1820, pp. 497–501, 2006, doi: 10.1007/1-4020-3920-4_32.

[19] B. Choudhury and A. Choudhury, "Dopant induced changes in structural and optical properties of Cr 3+ doped TiO2 nanoparticles," *Mater. Chem. Phys.*, vol. 132, no. 2–3, pp. 1112–1118, 2012, doi: 10.1016/j.matchemphys.2011.12.083.

[20] F. Malega, I. P. T. Indrayana, and E. Suharyadi, "Synthesis and Characterization of the Microstructure and Functional Group Bond of Fe3o4 Nanoparticles from Natural Iron Sand in Tobelo North Halmahera," *J. Ilm. Pendidik. Fis. Al-Biruni*, vol. 7, no. 2, pp. 129–138, 2018, doi: 10.24042/jipfalbiruni.v7i2.2913.

[21] A. Realpe Jimenez, D. Nuñez, N. Rojas, Y. Ramirez, and M. Acevedo, "Effect of Fe-N Codoping on the Optical Properties of TiO2for Use in Photoelectrolysis of Water," *ACS Omega*, vol. 6, no. 7, pp. 4932–4938, 2021, doi: 10.1021/acsomega.0c05981.

[22] C. Y. Wang, C. Böttcher, D. W. Bahnemann, and J. K. Dohrmann, "A comparative study of nanometer sized Fe(III)-doped TiO2 photocatalysts: Synthesis, characterization and activity," *J. Mater. Chem.*, vol. 13, no. 9, pp. 2322–2329, 2003, doi: 10.1039/b303716a.

[23] A. G. Akerdi, S. H. Bahrami, and E. Pajootan, "Modeling and optimization of Photocatalytic Decolorization of binary dye solution using graphite electrode modified with Graphene oxide and TiO2 03 Chemical Sciences 0306 Physical Chemistry (incl. Structural)," *J. Environ. Heal. Sci. Eng.*, vol. 18, no. 1, pp. 51–62, 2020, doi: 10.1007/s40201-019-00437-z.

[24] N. P. Sibiya, G. Amo-Duodu, E. K. Tetteh, and S. Rathilal, "Model prediction of coagulation by magnetised rice starch for wastewater treatment using response surface methodology (RSM) with artificial neural network (ANN)," *Sci. African*, vol. 17, p. e01282, 2022, doi: 10.1016/j.sciaf.2022.e01282.

[25] S. Kalikeri, N. Kamath, and D. J. Gadgil, "Visible light-induced photocatalytic degradation of Reactive Blue-19 over highly efficient polyaniline-TiO 2 nanocomposite : a comparative study with solar and UV photocatalysis," pp. 3731–3744, 2018.